http://dx.doi.org/10.5012/bkcs.2012.33.2.728

Dynamics of H Atom Production from Photodissociation of Formic Acid at 205 nm

Chan Ho Kwon, Mi Hyeon Choi, Hyonseok Hwang, and Hong Lae Kim*

*Department of Chemistry, College of Natural Sciences and Institute for Molecular Science and Fusion Technology, Kangwon National University, Chuncheon 200-701, Korea. *E-mail: hlkim@kangwon.ac.kr*
Received November 14, 2011, Accepted December 2, 2011

Key Words : Formic acid, Photodissociation dynamics, Laser induced fluorescence, H atoms

Chemistry of formic acid (HCOOH) is of fundamental interest because it is an important intermediate in oxidation of unsaturated hydrocarbons in combustion and the most abundant organic pollutant in Earth's atmosphere. Structures and dynamics of formic acid in the excited electronic states are of special importance in understanding atmospheric chemistry. In UV, the absorption spectrum shows some vibrational structures superimposed by continuous absorption starting from about 250 nm, which is assigned as the n $\rightarrow \pi^*_{C=O}$ electronic transition typical for simple carbonyl compounds.[1-3] The structures in this band are long progressions of the C=O stretching (ν_3) and the O-C-O bending (ν_7) vibrations resulting from structural changes from the planar to the pyramidal structure upon electronic transition due to molecular orbital interactions mentioned by Walsh.[4] Since the transition is vibronically allowed through ν_3 and ν_7, the direction of transition dipole moment has all three components in space expecting isotropic velocity distribution of fragments upon photodissociation.

Photodissociation of formic acid in the first UV absorption band has been extensively studied.[5-11] The major primary dissociation channel has been found to produce the CHO and OH radicals with quantum yield of 0.70 at 222 nm.[12] It was suggested that the dissociation should be predissociative and the potential energy surface leading to the CHO and OH radical products has an exit channel barrier. At the long-wavelength side of the absorption band (248 nm) where the photon energy is not high enough to overcome the barrier for dissociation on the S_1 excited state, the dissociation mainly takes place on the vibrationally hot ground electronic state after internal conversion producing CO, CO_2, and H_2O. As the photon energy increases, however, several dissociation channels in the excited electronic states are open such as CHO + OH and H atom production channels.

$$HCOOH + h\nu \rightarrow HCO + OH \quad \Delta H = 461.1 \text{ kJ/mol} \quad (1)$$
$$\rightarrow COOH + H \quad \Delta H = 377.0 \text{ kJ/mol} \quad (2)$$
$$\rightarrow HCOO + H \quad \Delta H = 467.0 \text{ kJ/mol} \quad (3)$$

Compared to the extensive studies on channel (1), the H atom production channels, (2) and (3) have not been investigated so far, whose quantum yield should be at least 0.3. The photophysical and photochemical processes from the ($n\pi^*$) state of HCOOH should depend upon the nature of the excited state and the shape of potential energy surfaces. In the present study, spectra of H atoms produced from photodissociation of HCOOH at 205 nm have been measured, from which the translational energy releases in the products are determined. In addition, the potential energy surfaces along the reaction coordinates leading to the H atom production channels have been constructed by quantum chemical calculations and the detailed dissociation dynamics for the channels (2) and (3) are discussed.

Experiments were performed in a low pressure flow-cell where the gaseous sample was slowly flowed through the cell at a pressure of about 50 mTorr from a reservoir that contained the liquid DCOOH and the vapor in equilibrium at ambient temperature. Spectra of H(D) atoms produced from photodissociation were measured by laser-induced fluorescence. The 205.14 nm light (205.09 nm for D atoms) induces the 1s $\rightarrow$ 3s, 3d transition by two photon absorption and fluorescence from the 3s $\rightarrow$ 2p transition at 656.6 nm (Balmer-α line) was detected. The 205.14 nm light was generated by mixing of the fundamental and the doubled output of a dye laser (Continuum ND-6000) in a BBO crystal, which was pumped by the second harmonic of an Nd:YAG laser (Continuum Surlite III). Within the same, ~8 nsec light pulse, the parent molecule absorbs a photon of energy high enough to produce H atoms, which results in the so-called one color experiment. The fluorescence was detected by a photomultiplier tube (Hammamatsu R-928) through a bandpass filter centered at 656 nm and the measured signal was recorded by a digital storage oscilloscope. The integrated signals were fed to a PC and the spectra were corrected by variation of the laser powers. The spectra of H atoms were measured in a linear regime of the log-log plot of the fluorescence signal vs. the laser power (slope ~3) with a properly chosen lens. The linewidth of the laser light was measured from the gaseous I_2 spectra near 615 nm, which was 0.09 cm^{-1} at FWHM. This laser line profile was deconvoluted from the measured Doppler profiles in the spectra to deduce the translational energies of the H atoms.

The spectra of H and D atoms produced from photodissociation of DCOOH are presented in Figure 1. As expected, the spectra show Gaussian-like profiles implying the isotropic velocity distribution of the photofragments as expected from the direction of the transition dipole moment. The Doppler broadened spectra are symmetrically extended from the center frequency, ν_0, which is 97,494 cm^{-1} in the present experiment, from $-\upsilon\nu_0/c$ to $+\upsilon\nu_0/c$ where c is the

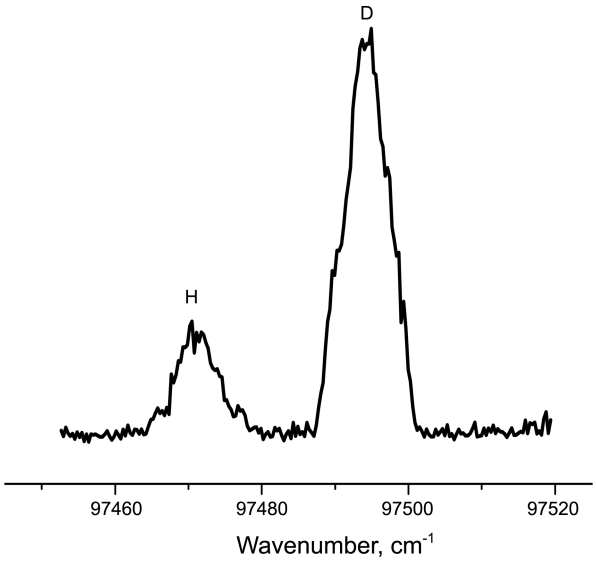

Figure 1. Laser induced fluorescence spectrum of H and D produced from photodissociation of DCOOH at 205 nm employing the 1s → 3s, 3d transition.

speed of light and υ is the magnitude of the velocity vector. The average relative translational energy of the two photofragments is obtained from the second moment of the excitation spectra using the formula

$$\langle E_T \rangle = \left(\frac{m_{RH}}{m_R}\right) \langle \left(\frac{\Delta \nu}{\nu_0}\right)^2 \rangle \frac{3}{2} m_H c^2$$

where m_H, m_{RH}, and m_R are the mass of the H atom, of the molecule being photodissociated, and of the partner fragment of the H atom, respectively. The spin-orbit couplings in the 3s and 3d state are neglected in obtaining the translational energies, because the experimental second moment is not accurate enough to justify the very small correction of the fine structure splitting (< 0.1 cm^{-1}). The measured center-of-mass translational energy releases for the channel (2) and (3) are 134.6 ± 16.8 and 113.9 ± 12.4 kJ/mol, respectively and listed in Table 1, which shows a large amount of the available energy is distributed into product translation. In addition, the D/H ratio was measured to be 2.7 ± 0.2 from the area of the peaks in the spectra implying the quantum yield of 0.22 and 0.08 for the channels (2) and (3), respectively.

The dynamics of dissociation should depend upon the shape of the potential energy surfaces leading to the individual product channels, which determines energy partitioning of the available energy into products. When the dissociation takes place along the repulsive surface, the dissociation is direct and fast where an impulsive dissociation model can be applied to obtain the energy partitioning. On the other hand, when the dissociation takes place on the ground electronic state after internal conversion upon excitation, the dissociation is slow where a statistical dissociation model such as a prior model can be applied. Although these are the two extreme cases, comparison of the experimental results with the calculated could provide an insight on the shape of the

Table 1. Translational energy releases (in kJ/mol) in products from photodissociation of DCOOH at 205 nm

		Exp	Impulsive	Prior	BIM[a]
E_{av}(C-D)[b]	205.6				
$\langle E_T$(C-D)$\rangle$		134.6 ± 16.8	184	56.0	138
E_{av}(O-H)[b]	115.6				
$\langle E_T$(O-H)$\rangle$		113.9 ± 12.4	111	25.5	108

[a]barrier impulsive model. [b]E_{av} = hν(205 nm) – D_0 (*Photochemistry of Small Molecules*; Okabe, H. Wiley: New York, 1978.)

potential energy surfaces. As the simple dissociation models, the impulsive model assumes an abrupt turn-on of the repulsive force between the separating atoms resulting in large translational energy release[13,14] whereas the prior model assumes statistical energy partitioning among all degrees of freedom of the products, namely translational, rotational, and vibrational degrees of freedom.[15,16] The calculated translational energy releases are listed in Table 1, where the experimental results are rather close to those of the impulsive dissociation model.

According to the spin correlation arguments, the two doublet product states should be correlated to the singlet and three triplet parent molecular states. Thus, the product channels should be correlated to either the ground S_0 or the triplet state because the excited S_1 state should be correlated to either one of the product should be on the excited electronic state. The H atom dissociation from formic acid should not occur on the ground singlet surface after the internal conversion judging from the observed translational energy releases. The triplet surface, however, would not be repulsive, either. Thus, the dissociation dynamics cannot be explained with the simple models mentioned above. In order to figure out the dissociation dynamics, the potential energy surfaces leading to the H atom channels were obtained by quantum chemical calculations employing the *Gaussian 09* program packages.[17] First, the optimized equilibrium geometries and energies on the ground state were obtained by density functional theory (DFT) calculations at the B3LYP/6-311++G(d,p) level. Then, the potential energies were calculated with geometry optimization as the C-D (O-H) bond distance extending up to 300 pm with 10 pm steps assuming the 300 pm distance is far enough for the two fragments to be separated. The potential energy surfaces on the triplet state were obtained by the same calculations as on the singlet state except for the spin multiplicity. The calculated potential energies along the reaction coordinates are presented in Figure 2. On the triplet surfaces along the reaction coordinates, energy barriers at the exit channels can be seen in the figure, that is the reverse, recombination barriers of 124.5 and 106.3 kJ/mol for the D and H atom channels, respectively. There would in general be no recombination barriers for simple bond fission reactions but in the case of dissociation on the excited states, the recombination barriers often exist due to structural changes in the course of reaction.[18-20] As can be seen in the figure, on the T_1 surface, OCO bond distances and angles change as the departing H atom moves

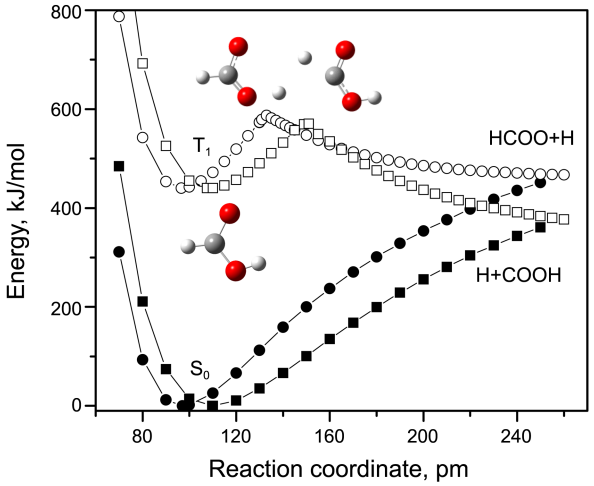

Figure 2. Potential energy curves along the reaction coordinates (the O-H and C-H bond distances) for the H atom production channels from formic acid, where circles and squares represent the HCOO + H and H + COOH channel, respectively. The filled symbols are for the S_0 state and the open symbols are for the T_1 state with molecular structures at equilibrium and on top of the barriers for both channels.

away for both the H and D atom channels compared to the equilibrium geometries. The barriers can also originate from the curve crossings in the excited electronic states but those cannot be distinguished because in the present study, the calculations are adiabatic. When the reverse barriers at the exit channel on the reaction coordinates exist, the energy partitioning of the available energy among the fragments would be determined at the exit channel. In this case, the energy partitioning can be modeled by the so-called "barrier impulsive model", where the dissociation impulsively takes place from the top of the barrier transforming the reverse barrier energy into product translation and the rest of the available energy would be statistically distributed among all degrees of freedom of the fragments. Thus, the translational energy of the fragments would be the sum of the translational energy from the impulsive model for the reverse barrier energy and that from the prior model for the rest of the available energy. Employing this model, the dissociation of hydrogen from ethylene,[21] OH from unsaturated alcohols,[22,23] and so forth could successfully be explained. The dissociation of H from formic acid in the present study can also be explained by this model, which provides the translational energy releases of 138 and 108 kJ/mol for the D and H atom channels, respectively. In the case of H from DCOOH, the excitation energy of 582.6 kJ/mol (205 nm) leads the parent molecule near the threshold of dissociation on the T_1 surface (near the forward barrier), which impulsively transforms almost all the available energy into product translation.

In summary, the H atoms are produced from photodissociation of formic acid along the T_1 surface via intersystem crossing from the S_1 initially excited state. The translational energy releases are determined at the exit channel where the barriers exist for both the C-H and O-H channels.

Acknowledgments. This work has been financially supported by National Research Foundation (2009-0072358) and Korea Research Foundation (331-2007-1-C00133).

References

1. Ng, T. L.; Bell, S. *J. Mol. Spectros.* **1974**, *50*, 166.
2. Demoulin, D. *Chem. Phys*. **1976**, *17*, 471.
3. Fridh, C. *J. Chem. Soc. Faraday trans. II* **1978**, *74*, 190.
4. Walsh, A. D. *J. Chem. Soc. (London)* **1953**, *1953*, 2306.
5. Ebata, T.; Fujii, A.; Amano, T.; Ito, M. *J. Phys. Chem*. **1987**, *91*, 6095.
6. Brouard, M.; O'Mahony, J. *Chem. Phys. Lett*. **1988**, *149*, 45.
7. Ebata, T.; Amano, T.; Ito, M. *J. Chem. Phys*. **1989**, *90*, 112.
8. Langford, S. R.; Batten, A. D.; Kono, M.; Ashfold, M. N. R. *J. Chem. Soc. Faraday Trans*. **1997**, *93*, 3757.
9. Shin, S. K.; Han, E. J.; Kim, H. L. *J. Photochem. Photobiol. A Chemistry* **1998**, *118*, 71.
10. Lee, K. W.; Lee, K. S.; Jung, K. H.; Volpp, H. R. *J. Chem. Phys*. **2002**, *117*, 9266.
11. He, H. Y.; Fang, W. H. *J. Am. Chem. Soc*. **2003**, *125*, 16139.
12. Singleton, D. L.; Paraskevopoulos, G.; Irwin, R. S. *J. Phys. Chem*. **1990**, *94*, 695.
13. Busch, G. E.; Wilson, K. R. *J. Chem. Phys*. **1972**, *56*, 3626.
14. Tuck, A. F. *J. Chem. Soc. Faraday Trans. II* **1977**, *73*, 689.
15. Zamir, E.; Levin, R. D. *Chem. Phys*. **1980**, *52*, 253.
16. Levin, R. D.; Bernstein, R. B. *Molecular Reaction Dynamics and Chemical Reactivity*; Oxford Univ. Press: New York, 1987.
17. *Gaussian 09*: Gaussian Inc.: Pittsburgh, PA, 2009.
18. Arunan, E.; Wategaonkar, S. J.; Setser, D. W. *J. Phys. Chem*. **1991**, *95*, 1539.
19. Dong, E.; Setser, D. W.; Hase, W. L.; Song, K. *J. Phys. Chem. A* **2006**, *110*, 1484.
20. Robinson, P. J.; Holbrook, K. A. *Unimolecular Reactions*; Wiley: New York, 1972.
21. Chang, A. H. H.; Hwang, D. W.; Yang, X. M.; Mebel, A. M.; Lin, S. H.; Lee, Y. T. *J. Chem. Phys*. **1999**, *110*, 10810.
22. Dhanya, S.; Kumar, A.; Upadhyaya, H. P.; Prakash, D. N.; Rameshwar, D. S. *J. Phys. Chem. A* **2004**, *108*, 7646.
23. Lee, J. H.; Hwang, H.; Kwon, C. H.; Kim, H. L. *J. Phys. Chem. A* **2010**, *114*, 2053.